Metal complexes of a new asymmetric hydrazonic ligand synthesis, characterization and microbicide activities

Abdou S. El-Tabl, Moshira M. Abd-El Wahed, Mohamad M. E. Shakdofa, Belal M. Herisha

Abstract-2,4-dihydroxy-2-hydroxybenzylidene) hydrazono)ethyl)phenyl) ethylidene)hydrazono)ethyl)-2,4-dihydroxyphenyl)ethan-1-one and its Fe(III), Co(II), Ni(II), Cu(II), Zn(II), Ag(I), Cd(II), Hg(II) and ZrO(II) complexes were synthesized and characterized by spectral and analytical techniques. The ligand binds the metal ions as a monobasic or neutral bidentate fashion via the protonated or deprotonated hydroxyl oxygen and azomethine nitrogen atom of salicyl moiety. All metal complexes are non-electrolytic in nature possessing a tetragonal distorted octahedral geometry. ESR spectral data of Cu(II) complexes are typical to d^9 configuration with an axial symmetry type of a $d_{(x2-y2)}$ ground state and a significantly covalent environment. The prepared compounds are more active against Fungi than bacteria. the promising active compounds against *A. flavus*, are **(1-6)** and **(11-14)** while complexes **(2-6), (8)** and **(11-13)** active against *S. cerevisiae*.

Index Terms: Metal complexes, Spectroscopic studies, Hydrazone, polydentate, Microbicide activities

1. INTRODUCTION

Polydentate hydrazonic ligands possess versatile coordination ability toward various transition metal ions. Hence, importance in the construction of metal complexes of several types. They have a key role in organic, inorganic and medicinal chemistry because of their structures [1, 2] and biological activity. Moreover, they are known to form stable complexes with different transition metal ions [3]. Hydrazone complexes of VO(II), Co(II), Ni(II), Cu(II) and Zn(II) were recently reported as antibacterial[4, 5] while complexes with Ni^{2+}, Cu^{2+} and Zn^{2+} were reported as antifungal.[6] In 2000 Y. Dong *et al*. reported a set of VO^{2+} complexes which have anti-leukemic activity.[7] Recently González-Baró et al. assayed the cytotoxicity activity of oxidovanadium(V) complexes with an Isonicotinohydrazide against the chronic myelogenous leukemia K562 cell line.[8] Because of hydrazoine ligand can have interesting biological activities and in continuation of our previous work, on the preparation of bioactive metal complexes.[3, 9-11]

This work redirected to prepare new polydentate hydrazonic ligand, 2,4-dihydroxy-2-hydroxybenzylidene) hydrazono)ethyl)phenyl)ethylidene) hydrazono)ethyl)-2,4-dihydroxyphenyl)ethan-1-one and its Fe^{3+}, Co^{2+}, Ni(II), Cu(II), Zn(II), Ag(II), Cd(II), Hg(II) and ZrO(II) complexes. The structure of the new compounds was studied by analytical and spectroscopic techniques. Moreover, the antimicrobial activity for the prepared compounds was evaluated against *A. flavus*, *S. cerevisiae*, *B. subtilis* and *E. coli* by disc-agar diffusion method.

- *Abdou S. El-Tabl, Professor at Chemistry Department, Faculty of Science, El-Menoufia University, Shebin El-Kom, Egypt*
- *Moshira M. Abd-El Wahed, Professor at Department of Pathology, Faculty of Medicine, El-Menoufia University, Shebin El-Kom, Egypt*.
- *Mohamad M. E. Shakdofa, professor at Chemistry Department, Faculty of Science and Arts, Khulais, University of Jeddah, Saudi Arabia*, *Inorganic Chemistry Department, National Research Center, El-bohouth St., Dokki, Cairo, Egypt*
- *Belal Herisha a graduate of Chemistry Department, Faculty of Science, El-Menoufia University, Shebin El-Kom, Egypt*

2. Experimental

2.1. Materials

All the reagents employed for the preparation of the ligand and its complexes were of the analytical grade available and used without further purification. 1,1'-(4,6-dihydroxy-1,3-phenylene)bis (ethan-1-one), hydrazine hydrate and 2-hydroxy benzaldehyde were provided from Sigma-Aldrich. DMF (assay 99.7%) and absolute ethanol (assay≥99.8%) were obtained from Sigma-Aldrich. The following reagents were obtained from Sigma-Aldrich: $Cu(CH_3COO)_2,H_2O$ (assay≥99%), $CuCl_2$ (assay≥99%), $Cu(NO_3)_2{\cdot}3H_2O$ (assay≥99.99%), $CuSO_4{\cdot}5H_2O$ (assay≥98%), $Ni(CH_3COO)_2{\cdot}4H_2O$ (assay≥99%), $Co(CH_3COO)_2.4H_2O$ (assay≥99.995%), (assay≥99%), $Zn(CH_3COO)_2{\cdot}2H_2O$ (assay≥99.99%), $FeCl_3{\cdot}6H_2O$ (assay≥97%), $Cd(CH_3COO)_2{\cdot}2H_2O$ (assay≥99.99%), $Hg(CH_3COO)_2.4H_2O$ (assay≥97%), $Ag(CH_3COO)$ (assay≥99%), $ZrOCl_2.8H_2O$(assay ≥99.5%), $NiSO_4{\cdot}7H_2O$ (assay≥99%), triethyl amine, TEA (assay 98%).

2.2. Physical Measurements

The ligand and its metal complexes were analyzed for C, H, N and Cl at the Micro-Analytical Laboratory, Cairo University, Egypt. Standard analytical methods were used to determine the metal ion content.[12-15] FT- IR spectra of the ligand and its metal complexes were measured using KBr discs with Jasco FT/IR 6100 type A infrared spectrophotometer covering the range 400-4000 cm^{-1}. The electronic absorption spectra of the investigated compounds were recorded on Unico 4802 UV/Vis. double beam spectrophotometer (190-1100 nm). The electronic absorption spectra of both ligand and its metal complexes were recorded using 1-cm quartz cells using

DMSO as a solvent. The thermal analysis (TG) was carried out on Shimadzu-50 thermal analyzer from room temperature to 800 ºC at a heating rate of 10 ºC/min. Magnetic susceptibilities were measured at 25ºC by the Gouy method using mercuric tetrathiocyanatocobaltate(II) as the magnetic susceptibility standard. Diamagnetic corrections were estimated from Pascal's constant.[16] The magnetic moments were calculated from the equation (1):

$$\mu_{eff} = 2.84\sqrt{\chi_M^{corr}} \cdot T \quad (1)$$

The molar conductivity of 10^{-3} M of metal complexes in dimethyl sulfoxide (DMSO) was determined using Jenway conductivity meter 4310 at room temperature. The molar conductivities were calculated according to the following equation (2):

$$\Lambda_M = \frac{V \times K \times Mw}{g \times \Omega} \quad (2)$$

where: Λ_M = molar conductivity / Ω^{-1} cm^2 mol^{-1}, V = volume of the complex solution/ mL, K = cell constant (0.92/ cm^{-1}), Mw = molecular weight of the complex, g = weight of the complex in gram, Ω = resistance. NMR spectrum was obtained on Brucker Avance 600-DRX spectrometers. ESR measurements of solid complexes at room temperature were made using Varian E-109 spectrophotometer, with DPPH as a standard material. TLC was used to confirm the purity of the prepared compounds.

2.3. *Synthesis of the ligand*

2.3.1. *Synthesis of 1-hydrazonoethyl)-2,4-dihydroxyphenyl)ethylidene)hydrazono)ethyl)-2,4-dihydroxyphenyl)ethan-1-one*

1-hydrazonoethyl)-2,4-dihydroxyphenyl)ethylidene)hydrazono)ethyl)-2,4-dihydroxyphenyl) ethan-1-one was prepared by refluxing 1'-(4,6-dihydroxy-1,3-phenylene)bis(ethan-1-one) (388 mg, 2.0 mmol) in 20 mL of absolute ethanol to hydrazine hydrate (100 mg, 2.0 mmol) (Fig. 1). The mixture was refluxed while stirring for 4 h. The solid product was filtered off, washed with cold ethanol, followed by crystallization from ethanol and finally dried under vacuum over anhydrous P_4O_{10}

2.3.2. *Synthesis of the ligand, (H_5L)*

The ligand, 2,4-dihydroxy-2-hydroxybenzylidene) hydrazono)ethyl)phenyl)ethylidene) hydrazono)ethyl)-2,4-dihydroxyphenyl)ethan-1-one (H_5L) was prepared by adding equimolar amounts of *1-hydrazonoethyl)-2,4-dihydroxyphenyl)ethylidene)hydrazono)ethyl)-2,4-dihydroxyphenyl) ethan-1-one* (398 mg, 1.0 mmol) in (50 mL) absolute ethanol to (122 mg, 1.0 mmol) of 2-hydroxy benzaldehyde in 20 mL absolute ethanol (Fig. 1). The mixture was refluxed while stirring for 3 h. The solid product was filtered off, washed with cold ethanol, followed by crystallization from ethanol and finally, dried under vacuum over anhydrous P_4O_{10}. Analytical and spectral data are given in Tables 1-2. (36.3 mg, 36.3 mmol, 80.0 %) as an olive solid, m.p. 260 °C. Elemental analysis for $H_5L(C_{27}H_{26}N_4O_6)$ (M. Wt. 502.53): Found (calcd) %C 64.15(64.53), %H 4.62(5.22), %N 10.68(11.15). IR (KBr, cm-1), 3555, 3480, 3405, 3240 ν(OH/H_2O), 1645 ν(C=O), 1620, 1605, 1570 ν(C=N), 1250 ν(C-O)$_{ph}$, 1045 ν(C-O)$_{Res}$. ^{1}H-NMR (600 MHz, DMSO-d$_6$): δ = 14.338, 14.042, 12.99, 11.137, 10.945 ppm (s, 5H, OH), 8.918 ppm (s, 1H, *H*-C^{26}=N^{14}), 2.668, 2.507 ppm ($^{15,16\&24}$CH$_3$&^{37}CH$_3$). ^{13}C-NMR (150 Mhz, DMSO-d6): 202.18 ppm (C^{35}=O^{36}), δ = 169.5, 166.07, 164.43, 159.66 (C-OH), 169.11, 157.86 ppm (C=N), 103.06-134.35 ppm (C-H)$_{ph}$, δ = 26, 14.3 ppm (CH$_3$)$_{Res}$. UV. vis. (1-cm quartz cells, DMSO) 260, 281, 310, 362 nm.

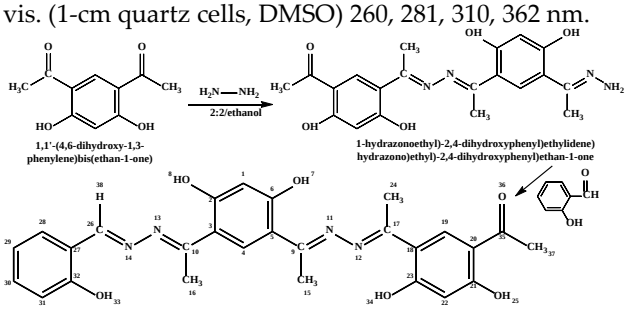

Fig. 1: Synthesis the ligand, 2,4-dihydroxy-2-hydroxybenzylidene)hydrazono)ethyl)phenyl)ethylidene)hydrazono)ethyl)-2,4-dihydroxyphenyl)ethan-1-one

2.4. *Synthesis of the metal complexes (2-14)*

2.4.1. *Synthesis of metal complexes (2), (7), (8), (10), (12) and (14)*

The metal complexes **(2), (7), (8), (10),** ***(12)*** and **(14)** were prepared by refluxing a hot ethanolic solution of the ligand (502 mg 1 mmol, 50 mL ethanol) with hot ethanolic solution of Cu(OAc)$_2$.H_2O (199.5 mg, 1 mmol) **(2),** Ni(OAc)$_2$.4H_2O (248.8 mg, 1 mmol) **(7),** Co(OAc)$_2$.4H_2O (249 mg, 1 mmol) **(8),** Zn(OAc)$_2$.2H_2O (220 mg, 1 mmol) **(10),** Hg(OAc)$_2$.4H_2O (318 mg, 1.0 mmol) **(12),** and $ZrOCl_2$.8H_2O (322.3 mg, 1 mmol) **(14)** respectively. The reaction mixtures were refluxed for 4 h. accompanied by stirring. 3 mL of diethyl amine were added to the reaction mixture in order to initiate precipitation of complexes**.** When the precipitate appeared, it was removed by filtration, washed with ethanol then by diethyl ether and dried in vacuum over P_4O_{10}. Analytical data are given in experimental part and table 1-2.

Cu(II) complex (2): Yield (74%), m.p. >300 ºC; color: dark olive; μ_{eff} = 1.77; molar conductivity (⌾$_m$): 3.8 ohm^{-1}cm^{2}mol^{-1}. Elemental analysis for [Cu(H_4L)(CH_3COO)(H_2O)$_2$], $C_{29}H_{32}N_4O_{10}Cu$, (660.14): Found (calcd) %C 52.8(52.76), %H 4.74(4.89), %N 9.15(8.49), %Cu 9.59(9.63). IR (KBr, cm^{-1}), 3560, 3475, 3415, 3240 ν(OH/H_2O), 1640 ν(C=O), 1620, 1607, 1565 ν(C=N), 1258 ν(C-O)$_{ph}$, 1043 ν(C-O)$_{Res}$, 1540/1435(Δ= 105) ν$_{s/as}$(CH_3COO), 525 ν(Cu-O), 470 ν(Cu-N). UV. vis. (1-cm quartz cells, DMSO) 270, 300, 390, 410, 435, 569, 1078 nm.

Ni(II) complex (7): Yield (68%), m.p. >300 ºC; color: olive; μ_{eff} = 3.84; molar conductivity (⌾$_m$): 6.2 ohm^{-1}cm^{2}mol^{-1}. Elemental analysis for [Ni(L)(CH_3COO)(H_2O)$_2$], $C_{29}H_{32}N_4O_{10}Ni$, (655.29): Found (calcd) %C 54.44(53.16), %H 4.81(4.92), %N 8.34(8.55), %Ni 8.74(9.21). IR (KBr, cm^{-1}), 3550, 3450, 3410, 3240 ν(OH/H_2O), 1641 ν(C=O), 1620, 1608, 1570 ν(C=N), 1255 ν(C-O)$_{ph}$, 1050 ν(C-O)$_{Res}$, 1547/1470(Δ= 77) ν$_{s/as}$(CH_3COO), 510 ν(Ni-O), 475 ν(Ni-N). UV. vis. (1-cm quartz cells, DMSO) 276, 290, 330, 360, 438, 620, 1060 nm.

Co(II) complex (8): Yield (75%), m.p. >300 ºC; color: brown; μ_{eff} = 4.98; molar conductivity (⌾$_m$): 6.3 ohm^{-1}cm^{2}mol^{-1}. Elemental analysis for [Co(H_4L)(CH_3COO)(H_2O)$_2$].H_2O, $C_{29}H_{34}N_4O_{11}Co$, (673.54): Found (calcd) %C 51.73(51.71), %H 4.74(5.09), %N 7.89(8.32), %Co 8.55(8.75). IR (KBr, cm^{-1}), 3550, 3480, 3410, 3230 ν(OH/H_2O), 1640 ν(C=O), 1620, 1608, 1572 ν(C=N), 1256 ν(C-O)$_{ph}$, 1048 ν(C-O)$_{Res}$, 1544/1440(Δ=

104) $\nu_{s/as}(CH_3COO)$, 555 ν(Co-O), 485 ν(Co-N). UV. vis. (1-cm quartz cells, DMSO) 263, 281, 320, 390, 477, 570, 1060 nm.

Zn(II) complex (10): Yield (78%), m.p. >300 °C; color: olive; molar conductivity (Ω_m): 3.5 $ohm^{-1}cm^2mol^{-1}$. Elemental analysis for $[Zn(H_5L)(CH_3COO)_2]$, $C_{31}H_{32}N_4O_{10}Zn$, (686.00): Found (calcd) %C 53.70(54.28), %H 4.76(4.70), %N 8.13(8.17), %Zn 8.89(9.53). IR (KBr, cm^{-1}), 3550, 3480, 3420, 3240 ν(OH/H_2O), 1645 ν(C=O), 1615, 1600, 1570, 1550 ν(C=N), 1265 $\nu(C\text{-}O)_{ph}$, 1045 $\nu(C\text{-}O)_{Res}$, 1530, 1420 (Δ= 110) $\nu_{s/as}(CH_3COO)$, 575 ν(Zn-O), 455 ν(Zn-N). UV. vis. (1-cm quartz cells, DMSO) 263, 288, 306, 373, 400 nm.

Hg(II) complex (12): Yield (75%), m.p. >300 °C; color: olive; molar conductivity (Ω_m): 2.3 $ohm^{-1}cm^2mol^{-1}$. Elemental analysis for $[Hg(H_4L)(CH_3COO)(H_2O)_2].H_2O$, $C_{29}H_{34}N_4O_{11}Hg$, (815.20): Found (calcd) %C 42.28(42.73), %H 3.34(4.20), %N 6.71(6.87), %Hg 24.00(24.61). IR (KBr, cm^{-1}), 3640, 3360, ν(OH/H_2O), 1645 ν(C=O), 1625, 1603, 1575 ν(C=N), 1270 $\nu(C\text{-}O)_{ph}$, 1042 $\nu(C\text{-}O)_{Res}$, 1560/1460 (Δ= 100) $\nu_{s/as}(CH_3COO)$, 525 ν(Hg-O), 505 ν(Hg-N). UV. vis. (1-cm quartz cells, DMSO) 264, 296, 340, 382, 425 nm.

ZrO(II) -complex (14): Yield (74%), m.p. >300 °C; color: brown; molar conductivity (Ω_m): 6.6 $ohm^{-1}cm^2mol^{-1}$. Elemental analysis for $[ZrO(H_4L)(Cl)(H_2O)_{0.5}]$, $C_{27}H_{26}N_4O_{7.5}ZrCl$, (653.20): Found (calcd) %C 49.41(49.65), %H 4.33(4.01), %N 8.11(8.58), %Zr 5.04(5.43). IR (KBr, cm^{-1}), 3550, 3450, 3410, 3240 ν(OH/H_2O), 1643 ν(C=O), 1620, 1605, 1570 ν(C=N), 1268 $\nu(C\text{-}O)_{ph}$, 1046 $\nu(C\text{-}O)_{Res}$, 950 ν(Cl), 550 ν(Zr-O), 495 ν(Zr-N). UV. vis. (1-cm quartz cells, DMSO) 269, 277, 337, 377, 403 nm.

2.4.2. Synthesis of metal complexes (3-6), (9), (11) and (13)

The metal complexes **(3-6), (9), (11)** and **(13)** were prepared by refluxing a hot ethanolic solution of the ligand (1004 mg 2 mmol, 50 mL ethanol) with hot ethanolic solution of $CuCl_2.2H_2O$ (170 mg, 1 mmol) **(3),** $Cu(SO_4)_2.5H_2O$ (245 mg, 1 mmol) **(4),** $Cu(NO_3)_2.3H_2O$ (241 mg, 10 mmol) **(5),** $Ni(SO_4.7H_2O$ (262.9 mg, 1 mmol) **(6),** $FeCl_3.6H_2O$ (270.3 mg, 1 mmol) **(9),** $Cd(OAc)_2.2H_2O$ (267 mg, 1 mmol) **(11)** and Ag(OAc) (166.9 mg, 1 mmol) **(13)** respectively. The reaction mixtures were refluxed for 4 h. accompanied by stirring. 3 mL of triethyl amine were added to the reaction mixture in order to initiate precipitation of complexes**.** When the precipitate appeared, it was removed by filtration, washed with ethanol then by diethyl ether and dried in vacuum over P_4O_{10}. Analytical data are given in experimental part.

Cu(II) complex (3): Yield (69%), m.p. >300 °C; color: olive; μ_{eff} = 1.87; molar conductivity (Ω_m): 5.0 $ohm^{-1}cm^2mol^{-1}$. Elemental analysis for $[Cu(H_4L)_2(H_2O)_2]$, $C_{54}H_{54}N_8O_{14}Cu$, (1102.61): Found (calcd) %C 59.53(58.82), %H 4.85(4.96), %N 10.23(10.16), %Cu 5.99(5.86). IR (KBr, cm^{-1}), 3610, 3240 ν(OH/H_2O), 1645 ν(C=O), 1615, 1607, 1575 ν(C=N), 1269 $\nu(C\text{-}O)_{ph}$, 1047 $\nu(C\text{-}O)_{Res}$, 580 ν(Cu-O), 460 ν(Cu-N). UV. vis. (1-cm quartz cells, DMSO) 266, 289, 351, 400, 450, 517, 1078 nm.

Cu(II) complex (4): Yield (77%), m.p. >300 °C; color: brown; μ_{eff} = 1.99; molar conductivity (Ω_m): 15.5 $ohm^{-1}cm^2mol^{-1}$. Elemental analysis for $[Cu(H_5L)_2(SO_4)(H_2O)].4H_2O$, $C_{54}H_{62}N_8O_{21}CuS$, (1254.73): Found (calcd) %C 51.81(51.69), %H 4.71(4.98), %N 9.00(8.95), %Cu 4.71(5.06). IR (KBr, cm^{-1}), 3600, 3320 ν(OH/H_2O), 1645 ν(C=O), 1615, 1570 ν(C=N), 1270 $\nu(C\text{-}O)_{ph}$, 1045 $\nu(C\text{-}O)_{Res}$, 1138, 1070, 900 $\nu(SO_4)$, 555 ν(Cu-O), 485 ν(Cu-N). UV. vis. (1-cm quartz cells, DMSO) 277, 297, 387, 434, 600, 1072 nm.

Cu(II) complex (5): Yield (75%), m.p. >300 °C; color: brown; μ_{eff} = 2.18; molar conductivity (Ω_m): 11.9 $ohm^{-1}cm^2mol^{-1}$. Elemental analysis for $[Cu(H_5L)_2(NO_3)_2]$, $C_{54}H_{52}N_8O_{18}Cu$, (1192.61): Found (calcd) %C 55.03(54.38), %H 4.96(4.40), %N 10.55(11.74), %Cu 4.81(5.33). IR (KBr, cm^{-1}), 3560, 3480, 3420, 3240 ν(OH/H_2O), 1645 ν(C=O), 1620, 1570 ν(C=N), 1268 $\nu(C\text{-}O)_{ph}$, 1045 $\nu(C\text{-}O)_{Res}$, 1455, 1360, 950 $\nu(NO_3)$, 555 ν(Cu-O), 485 ν(Cu-N). UV. vis. (1-cm quartz cells, DMSO) 260, 281, 310, 362, 490, 635, 1060 nm.

Ni(II) complex (6): Yield (78%), m.p. >300 °C; color: olive; μ_{eff} = 3.56; molar conductivity (Ω_m): 30.7 $ohm^{-1}cm^2mol^{-1}$. Elemental analysis for $[Ni(H_5L)_2(SO_4)(H_2O)]$, $C_{54}H_{54}N_8O_{17}NiS$, (1177.82): Found (calcd) %C 54.63(55.07), %H 4.43(4.62), %N 9.11(9.51), %Ni 4.89(4.98). IR (KBr, cm^{-1}), 3555, 3470, 3420, 3230 ν(OH/H_2O), 1638 ν(C=O), 1621, 1611, 1573 ν(C=N), 1261 $\nu(C\text{-}O)_{ph}$, 1049 $\nu(C\text{-}O)_{Res}$, 1115, 1049, 880 $\nu(SO_4)$, 576 ν(Ni-O), 479 ν(Ni-N). UV. vis. (1-cm quartz cells, DMSO) 263, 288, 326, 383, 500, 650, 1085 nm.

Fe(III) complex (9): Yield (78%), m.p. >300 °C; color: brown; μ_{eff} = 5.44; molar conductivity (Ω_m): 17.2 $ohm^{-1}cm^2mol^{-1}$. Elemental analysis for $[Fe(H_4L)_2(Cl)(H_2O)]$, $C_{54}H_{52}N_8O_{13}ClFe$, (112.35): Found (calcd) %C 57.76(58.31), %H 4.92(4.71), %N 10.00(10.07), %Cl 2.75(3.19), %Fe 5.89(5.02). IR (KBr, cm^{-1}), 3530, 3460, 3410 ν(OH/H_2O), 1640 ν(C=O), 1620, 1607, 1570 ν(C=N), 1267 $\nu(C\text{-}O)_{ph}$, 1047 $\nu(C\text{-}O)_{Res}$, 577 ν(Fe-O), 465 ν(Fe-N). UV. vis. (1-cm quartz cells, DMSO) 255, 285, 340, 380, 470, 540, 880 nm.

Cd(II) complex (11): Yield (79%), m.p. >300 °C; color: olive; molar conductivity (Ω_m): 4.2 $ohm^{-1}cm^2mol^{-1}$. Elemental analysis for $[Cd(H_4L)_2]$, $C_{54}H_{50}N_8O_{120}Cd$, (1115.45): Found (calcd) %C 58.78(58.15), %H 4.78(4.52), %N 9.83(10.05), %Cu 9.88(10.08). IR (KBr, cm^{-1}), 3600, 3320 ν(OH/H_2O), 1645 ν(C=O), 1617, 1602, 1578, 1558 ν(C=N), 1271 $\nu(C\text{-}O)_{ph}$, 1043 $\nu(C\text{-}O)_{Res}$, 590 (Cd-O), 515 ν(Cd-N), ^{1}H-NMR (600 MHz, DMSO-d_6): δ = 13.432, 11.02, 10.645, ppm (s, 4 H, OH), 8.633 ppm (s, 1H, *H*-C^{26}=N^{14}), 2.721, 2.543 ppm ($^{15,16\&24}CH_3\&^{37}CH_3$). UV. vis. (1-cm quartz cells, DMSO) 264, 286, 308, 380, 410 nm.

Ag(I) complex (13): Yield (70%), m.p. >300 °C; color: olive; molar conductivity (Ω_m): 2.3 $ohm^{-1}cm^2mol^{-1}$. Elemental analysis for $[Ag(H_5L)_2(CH_3COO)(H_2O)]$, $C_{56}H_{55}N_8O_{14}Ag$, (1171.97): Found (calcd) %C 57.05(57.39), %H 4.64(4.73), %N 8.95(9.56), %Ag 8.83(9.20). IR (KBr, cm^{-1}), 3555, 3480, 3410, 3210 ν(OH/H_2O), 1642 ν(C=O), 1618, 1607, 1565, 1555 ν(C=N), 1270 $\nu(C\text{-}O)_{ph}$, 1045 $\nu(C\text{-}O)_{Res}$, 1539, 1420(Δ= 119) $\nu_{s/as}(CH_3COO)$, 557 ν(Ag-O), 457 ν(Ag-N). UV. vis. (1-cm quartz cells, DMSO) 270, 285, 336, 364, 395 nm.

2.5. Biological activities

Antimicrobial activities of the synthesized compounds (**1-14**) were evaluated against a panel of microorganisms in comparison with both positive controls (nystatin for fungi, tetracycline for bacteria) and negative controls (solvent, DMSO) as well as metal salt solutions. Microorganisms used were Gram positive bacteria (*Bacillus*

subtilis), Gram-negative bacteria, *Escherichia coli* (*E. coli*) and fungi, *Aspergillus flavus (A. flavus)* and *Saccharomyces cerevisiae (S. cerevisiae).* All microorganisms used were obtained from the culture collection of Lab. of microbiology, Biology Department, Faculty of Science and Arts, University of Jeddah, KSA. The microorganisms were passaged at least twice to ensure purity and viability. The compounds were mounted on a concentration of 100 µg/disc. The bacteria were maintained on nutrient agar medium while yeast and fungi were maintained on Czapek Dox´s agar medium. DMSO showed no inhibition zone was used as a negative control. The agar media were incubated with different microorganism cultures tested. After 24 h of incubation at 37 °C for bacteria and yeast and 72 h of incubation at 28 °C for *A. flavus*, the diameter of inhibition zone in mm was measured. Tetracycline and nystatin were used as a positive control for antimicrobial activity at concentration of 100 µg/disc.

2.5.1. Preparation of the discs

Compounds (**1-14)** together with the positive control (tetracycline, nystatin) were mounted on a paper disc prepared from blotting paper (5 mm diameter) with the help of a micropipette in a concentration of 100 µg/disc. The discs were applied on the microorganism-grown agar plates.

2.5.2. Preparation of agar plates

Minimal agar was used for the growth of specific microbial species. The preparation of agar plates for *Bacillus subtilis*, and *Escherichia coli* (bacteria) utilized nutrient agar (2.30 g/ 100 ml distilled water) and Czapek Dox´s agar medium (3.9 g/100 ml distilled water) for *A. flavus* and *S. cerevisiae* (fungi). This could soak for 15 min and then boiled on a water bath until the agar was completely dissolved. The mixture was autoclaved for 15 min at 120 °C and then poured into previously sterilized Petri dishes and stored at 30 °C for inoculation.

2.5.3. Inoculation procedure

Spore suspension was prepared with the help of a platinum wire loop to reach a microbial concentration equivalent 0.5 Mac-Farland.

2.5.4. Application of the discs

Sterilized forceps were used for the application of the paper disc on previously inoculated agar plates. When the discs were applied, they were incubated at 37 °C for 24 h for bacteria and yeast, and at 28 °C for 48 h for fungi. The zone of inhibition around the disc was then measured in millimeters. The activity index for the complexes was calculated by following formula.[6]

$$Activity\ index = \frac{Diameter\ of\ inhibation\ zone\ by\ test\ compound}{Diameter\ of\ inhibation\ zone\ by\ standard} \times 100$$

3. RESULTS AND DISCUSSION

The reaction of ligand **(1)** with metal salts in mole ratios (1L: 1M) or (2L: 1M) gave complexes; (**2-14)**. All metal complexes are colored, solids, and stable in ordinary conditions and don't decompose after elongated storage at room temperature. The complexes are insoluble in solvents H_2O, EtOH, MeOH, $C_6H_5CH_3$, CH_3CN and $CHCl_3$, but completely soluble in both dimethylformamide (DMF) and dimethyl sulfoxide (DMSO). Elemental analyses, physical and spectral data are presented in experimental part. The analyses data agree with the assumed formula illustrated in Figs. 2-6. The elemental analyses confirmed that, the complexes **(2), (7), (8), (10), (12)** and **(14)** were found to be formed in 1L:1M molar ratio while complexes **(3-6), (9), (11)** and **(13)** were found to be formed in molar ratio 2L:1M.

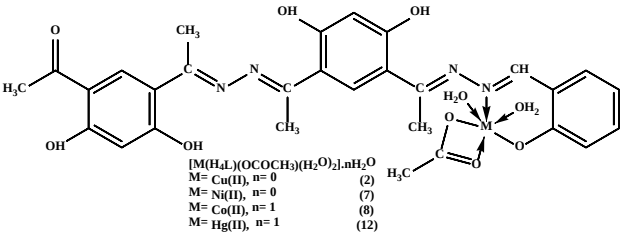

Fig. 2: Structure representation of Cu(II), Ni(II), Co(II) and Hg(II) complexes (2), (7-8) and (12)

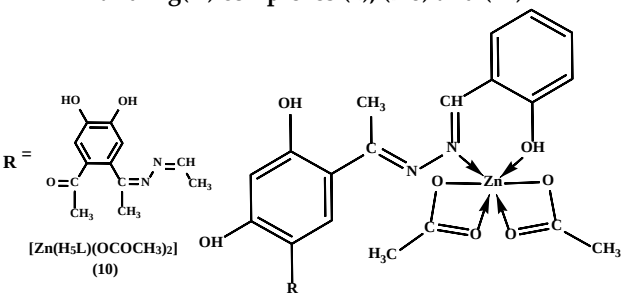

Fig. 3: Structure representation of Zn(II)complex (10)

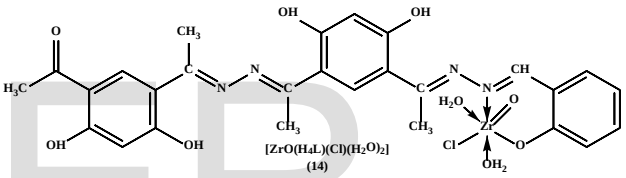

Fig. 4: Structure representation of ZrO(II) complex (14)

3.1. Molar conductivity

The molar conductivity of 1×10^{-3} M solution of the metal complexes **(2-14)** in DMF at room temperature are given in experimental part. The values of molar conductance of all complexes are in the 2.3-30.7 Ω^{-1} cm^2 mol^{-1} range which is within the expected range of (1–35 $ohm^{-1}cm^2mol^{-1}$) for the complexes to behave as nonelectrolytes. These findings confirm the non-electrolytic nature of these complexes and support that, the anions are coordinated to metal ion in these complexes.[17] The considerably high values of some complexes may be due to the partial solvolysis by DMF.[17]

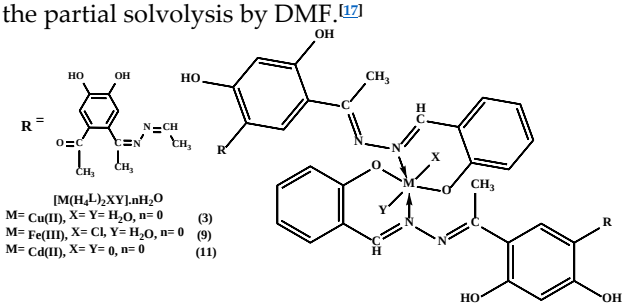

Fig. 5: Structure representation of Cu(II), Fe(III), Zn(II) and Cd(II) complexes (3) and (9) and (11)

IJSER

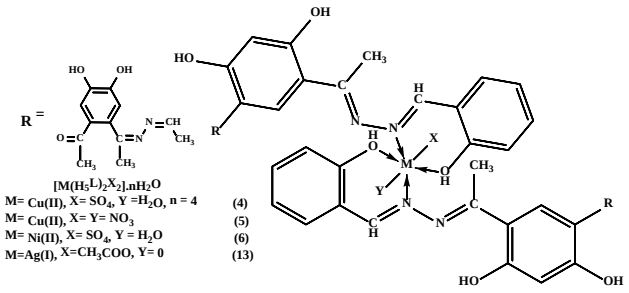

Fig. 6: Structure representation of Cu(II), Ni(II), Tl(I) and Ag(I) complexes (4-6) and (13)

3.2. Nuclear magnetic resonance spectrum

3.2.1. ^{1}H- NMR spectrum

The observed ^{1}H- and ^{13}C- chemical shifts of the ligand **(1)** in DMSO-d_6 are presented in experimental part. The ligand ^{1}H-NMR spectrum is compatible with the proposed structure as shown in Fig. 1. The signals observed as singlet at 14.338, 14.042, 12.99, 11.137 and 10.945 ppm (s, 1H, O*H*) were assigned to the hydroxyl protons of resorcinol and salicyl moieties. The considerable high δ values of these hydrogen chemical shifts is related to the proton-attachment to high electronegative atoms (oxygen). This assignment is supported by the apparent intensity decreased of these signals in the deuterated ligand spectrum. While the singlet observed at 8.918 ppm is attributed to the azomethine proton (s, 1H, *H*-C^{26}=N^{14}). The positions of these signals in the downfield region as well as the broadening of OH signal suppose the presence of a considerable extent of hydrogen bonding. While the chemical shift of the aromatic protons was observed in the range 6.391-8.2312 [18-20]. Finally, the singlet peaks observed at δ = 2.668 and 2.507 ppm were assignable to the methyl group protons ($^{15,16\&24}$CH$_3$&^{37}CH$_3$). By comparison of the ^{1}H- NMR of the ligand and that of the Cd(II) complex **(11)**, it was found that the signal of hydroxyl proton of the salicyl moiety disappeared indicating that, the ligand bonded to the Cd(II) ion by the deprotonated hydroxyl group of salicyl moiety. In addition, there is a significant downfield shift of the azomethine proton signal in the complexes relative to the free ligand that indicates the coordination of the azomethine nitrogen atom. This is may be due to the donation of the lone pair of electrons of nitrogen to the central metal atom resulting in the formation of a coordinated bond (N→M).[21, 22]

3.2.2. ^{13}C- NMR spectrum

The ligand ^{13}C-NMR spectrum showed a signal at 202.18 ppm which could be assigned to carbonyl group (C^{35}=O^{36}). The chemical shift which observed at δ = 169.5, 166.07, 164.43, 159.66 were attributed to the carbon atoms attached to the hydroxyl groups.[20] Whereas the chemical shift appeared at 169.11 and 157.86 ppm were attributed the carbon atoms of azomethine groups. While the chemical shifts appeared in the 103.06-134.35 ppm range were assignable to the aromatic proton of resorcinol and salicyl moieties. The chemical shift appearing at 26 and 14.3 ppm could be attributed to the methyl carbon atoms of resorcinol moiety.

3.3. Mass spectra of the ligand

The mass spectrum of the ligand supports its suggested structure. It reveals molecular ion peak m/z at 502 is consistent with the molecular weight of the ligand. Moreover, the mass spectrum of ligand showed several fragments which possessed ion peaks in the range 398- 485 due the elimination of hydroxyl and/or methyl groups. In addition, there are many main peaks with molecular ions peaks equal to m/z= 382, 310, 192, 161, 150, 135, 120, 93 and 77 which corresponding to $C_{20}H_{20}N_3O_4$, $C_{17}H_{16}N_3O_3$, $C_{10}H_{10}NO_3$, $C_9H_9N_2O$, $C_8H_8NO_2$, $C_7H_5NO_2$, C_7H_6NO, C_6H_5O and C_6H_5 respectively. The mass spectrum of Zn(II) complex **(10)** support their proposed structure. It shows molecular ion peaks m/z at 686 consistent with its molecular weight.

3.4. Infrared spectra (IR)

The IR spectrum of the ligand and its metal complexes are listed in experimental part. The spectrum of ligand showed a band at 1645 cm^{-1} which may be attributable to the carbonyl group of resorcinol moiety ν(C=O), while the week and broad bands which observed in the 3240-3555 cm^{-1} range is attributable to the stretching vibration of the hydroxyl group of resorcinol and salicyl moieties associated in an inter- and intermolecular hydrogen bonding.[23-29] The spectrum of the ligand also showed bands in the range 1620-1570 cm^{-1} which may be assignable to azomethine ν(C=N) and aromatic ν(C=C) groups. In addition, the bands which appeared at 1250, 1045 may be assignable to the phenolic ν(C-OH) of the salicyl[29, 30] and resorcinol[31, 32] moieties respectively. The chelation mode of the ligand can be established by comparing the infrared spectra of complexes with that of the free ligand. This comparison showed that, the ligand acts as a neutral or monobasic bi-dentate agent bonding to metal ions through oxygen atom of protonated or deprotonated hydroxyl group and azomethine nitrogen atom of the salicyl moiety, the following evidences proposed this bonding mode: i) The higher shift of phenolic C–O band of salicyl moiety with respect to the spectrum of the parent ligand and appeared in the 1255-1271 cm^{-1} range. ii) There is a significant downfield shift of the azomethine proton signal in the ^{1}H-NMR spectrum of Cd(II) complex relative to the free ligand that indicates the coordination of the azomethine nitrogen atom of salicyl moiety with metal ions. iii)The disappearance of the signal characteristic to the hydroxyl group proton of salicyl moiety in the ^{1}NMR spectrum of Cd(II) complex **(11)** confirmed that, the monobasic nature of the ligand. iv) The presence of new bands in the 457-590 cm^{-1} range could be attributed to the metal bond with oxygen and nitrogen atoms. In the acetate complexes, the acetate may be coordinated to the metal ion in unidentate, bidentate or bridging bidentate manner. The $\nu_{as}(CO_2^-)$ and $\nu_s(CO_2^-)$ of the free acetate ion are at *ca*. 1560 and 1416 cm^{-1} respectively. In the unidentate acetate complexes, ν(C=O) was higher than $\nu_s(CO_2^-)$ and ν(C–O) was lower than $\nu_{as}(CO_2^-)$. As a result, the separation between the two peak was much larger in the unidentate than in the free ion but in the bidentate, the separation was lower than in the free ion while in the bridging bidentate, the two ν(CO) were closer to the free ion.[33] In the acetate complexes **(2), (7-8), (10), (12)** and **(13),** the appearing of two bands in the 1539-1560 cm^{-1} and 1420-1470 cm^{-1} ranges were imputed to $\nu_{as}(COO^-)$

and $\nu_s(COO^-)$, respectively, stating the involvement of the acetate oxygen in the chelation. The difference magnitude (Δ) between $\nu_{as}(CO_2^-)$ and $\nu_s(CO_2^-)$ in these complexes were in the range 77-119 cm^{-1} implying that acetate group was chelated as a bidentate fashion.[10, 34] The sulfato complex **(4)** and **(6)** revealed bands at 1138, 1070 and 900; 1115, 1049 and 880 cm^{-1} characteristics for the coordinated sulphate group which was further confirmed by their low conductance values.[33, 35] The nitrate ions (NO_3) can coordinate to a metal ion as a unidentate, symmetric, and asymmetric chelating bidentate, and bridging bidentate ligand of various structures. It is rather difficult to differentiate these structures by vibrational spectroscopy since the symmetry of the nitrate ion differs very little among them (C_{2v} or C_s). Even so, vibrational spectroscopy is still useful in distinguishing unidentate and bidentate ligands.[33] Originally, Gatehouse et al.[36] noted that the unidentate NO_3 group exhibits three NO stretching bands, as expected for its C_{2v} symmetry. The IR spectrum of the nitrato complex **(5)** showed bands at ν_5(1455), ν_1(1360) and ν_2(950) indicating the nitrate group coordinated to the metal ion. The difference between the two high bands (ν_5-ν_1) is 95 cm^{-1} indicating that, the nitrate ion bonded to the Cu(II) ion is unidentate manner.[33, 37, 38] In case of ZrO(II) complexes **(14),** it can be noted that, there is a new band at 950 cm^{-1} for this complex, which attributable to ν(Zr=O).[39] The spectral results together with elemental analysis indicates that, the ligand acted as a neutral bidentate or monobasic bidentate fashion bind to metal ions via oxygen atom of protonated or deprotonated hydroxyl group and azomethine nitrogen atom of the salicyl moiety.

3.5. Electronic absorption spectra and magnetic moments measurements

The electronic spectra of the ligand **(1)** and its metal complexes **(2-14)** were carried out in DMF and their data are listed in experimental part. The spectrum of the ligand showed four bands at 260, 281, 310 and 362 nm. The first two bands of shortest wavelength may be assignable to the $\pi\rightarrow\pi^*$ transition in the benzenoid moieties and intra ligand $\pi\rightarrow\pi^*$ transition. However, the third and fourth peaks could be attributed to $n\rightarrow\pi^*$ transition of azomethine and carbonyl groups. The metal complexes spectra showed that, the bands characteristic to n-π^* transitions were shifted to some extent, probably due to the chelation of carbonyl and azomethine groups to the metal ion.[40, 41] The absorption spectra of six-coordinate Cu(II) complexes are analyzed assuming D_4 or C_{4v} symmetry, the e_g and t_{2g} levels of the ^2D free ion term are further split into B_{1g}, A_{1g}, B_{2g} and E_g levels, respectively. Thus, three spin allowed transitions are expected in the visible and near IR region of copper(II) and such bands are resolved by Gaussian analysis and analyzed by single crystal polarization studies and are assigned to the $(\nu_1)^2B_{1g}\rightarrow{}^2A_{1g}(d_{x2-y2}\rightarrow d_{z2})$; $(\nu_2)^2B_{1g}\rightarrow{}^2B_{2g}$ $(d_{x2-y2}\rightarrow d_{xy})$ and $(\nu_3)^2B_{1g}\rightarrow{}^2B_g(d_{x2-y2}\rightarrow d_{xz},d_{yz})$ transitions in order of increasing energy. The energy level sequence will depend on the amount of distortion, due to ligand field and Jahn-Teller effect. The electronic spectra of the copper complexes **(2-5)** displays three bands in the 1060-1078, 517-635, 435-490 nm ranges which may assumable to ν_1, ν_2 and ν_3 respectively indicate that these complexes may be have a tetragonal distorted octahedral geometry.[42-45] The electronic absorption spectra of Ni(II) complexes **(6)** and **(7)** are consistent with an octahedral stereochemistry around the nickel(II) ion, showing transition bands at 500, 650, 1085 and 438, 620, 1060 nm. These are assignable to the transitions $^3A_{2g}(F)\rightarrow{}^3T_{2g}(F)$, $^3A_{2g}(F)\rightarrow{}^3T_{1g}(F)$, $^3A_{2g}(F)\rightarrow{}^3T_{1g}(P)$ respectively.[45, 46] The ν_2/ν_1 ratio of these complex are 1.71 and 1.67 which is close to the usual range 1.50–1.75, consistent with its octahedral stereochemistry Ni(II) complex [47]. Co(II) complex **(8)** electronic spectrum shows electronic spectral bands at 477, 570, 1060 nm corresponding to the transitions $^4T_{1g}(F)\rightarrow{}^4T^2{}_g(F)$, $^4T_{1g}(F)\rightarrow{}^4A_{2g}(F)$ and $^4T_{1g}(F)\rightarrow{}^4T_{1g}(P)$ suggesting a six-coordinated octahedral geometry.[45, 48-51] The ratio of ν_2/ν_1 is 1.86, lower than for an octahedral cobalt(II) (1.95–2.48), indicates distorted octahedral structure. This is consistent with very broad nature of the band which may be assigned to the envelope of the transitions from $^4E_g(^4T_{1g})$ to the components $^4B_{2g}$ and ^4E_g of $^4T_{2g}$ characteristic of tetragonally-distorted octahedral environment.[45, 48-51] The Fe(III) complex **(9)** spectrum showed two bands at 470, 540nm and a shoulder at 880 nm attunable to $(\nu_1)^6A_{1g}(S)\rightarrow{}^4T_{1g}(G)$, $(\nu_2)^6A_{1g}(S)\rightarrow{}^4T_{2g}(G)$ and $(\nu_3)^6A_{1g}(S)\rightarrow{}^4A_{1g}(G),{}^4E_g(G)$ transitions suggesting octahedral geometry around the Fe(III) ions.[45, 46, 52] Zn(II), Cd(II), Ag(I) and Hg(II) complexes **(10-14)** showed diamagnetic character as expected. They do not show any transitions, and the observed bands are only intra-ligand transitions [53, 54]. Their structures suggested based on the analytical and thermal analysis and are most probably hexacoordinate of tetracoordinate.

3.6. Magnetic susceptibility

The corrected magnetic moments were calculated from the molar magnetic susceptibility values, using Pascal's constants.[55] The magnetic moments values for the paramagnetic complexes **(2-9)** are presented in experimental part and its magnitudes fall within the ranges associated with spin-free high spin ions in octahedral or square pyramidal fields. The Cu(II) complexes **(2-5)** magnetic moment values at room temperature are in the 1.77-2.18 BM which is corresponding to one unpaired electron usually observed for mononuclear Cu(II) complexes, regardless of stereochemistry. The Ni(II) complex **(6-7)** gave magnetic moment equal to 3.56 and 3.84 BM characteristic of two unpaired electrons system. The Co(II) complex **(8)** has a magnetic moment of 4.98 BM which is higher than the spin-only value and a typical value of a d^7 system with three unpaired electrons indicating a quartet state in an octahedral arrangement around the metal, as compared with the reported values for octahedral Co(II) complexes of (4.7–5.2 BM).[32, 46] The Fe(III) complex **(9)** gave magnetic moment value 5.44 BM respectively, compatible with high spin d^5 Fe(III) ion.[56]

3.7. ESR of copper(II) complexes

ESR spectra of copper(II) complexes give more information about the bonding site and geometry of the complexes. It was recorded in polycrystalline state at room temperature on X-band at frequency 9.8 GHz and their data listed in Table 1. The ESR spectra of the solid Cu(II) complexes **(2-4)** exhibited anisotropic signals with $g_{\parallel}$, $g_{\perp}$ and g_{iso} values are in the 2.248-2.277, 2.045-2.05 and

2.112-2.124 ranges respectively. These values are typical for a species d^9 configuration with an axial symmetry type of d_{x2-y2} ground state. $g_{\parallel}$ and $g_{\perp}$values are close to 2.00 and $g_{\parallel}>g_{\perp}>g_e$(2.0023), stating that all these complexes have a distorted octahedral structure.[57-59] With respect to Hathaway expression which stated that G= $(g_{\parallel}-2)/(g_{\perp}-2)$, the exchange coupling interaction between Cu(II) ions is negligible if G>4 whereas a considerable interaction is present if G<4.[60, 61] The G values of our complexes are in the 5.27-5.90 range [Table 1], indicating that, the interaction between Cu(II) ions is negligible.[60] The index of tetragonal distortion f is calculated as $f = g_{\parallel}/A_{\parallel}$ and depending on the nature of the coordinated atom.[62] If the value ranged from 105 to 135 the geometry is square-planar while if it is ranged from 150 to 250 the geometry is tetrahedrally distorted octahedral 150-250 cm^{-1}. The $g_{\parallel}/A_{\parallel}$ for complexes **(2-4)** are in the 164.7-178.5 confirmed that the geometry of Cu(II) complexes **(2-4)** are tetragonally distorted octahedral.[34, 47] Kivelson and Neiman show that the $g_{\parallel}$-values in the Cu(II) complexes can be used as a measure of covalent character of the metal–ligand bond. If this value is greater than 2.3, the environment is essentially ionic but if the value less than this limit indicate a covalent environment.[63] The $g_{\parallel}$-values reported here are in the 2.248-2.277 range, indicating that, there is a considerable covalent bonding character in these complexes [34]. The g-values can be related to the parallel ($K_{\parallel}$) and perpendicular ($K_{\perp}$) components of the orbital reduction factor (K) as following equations (3-5).[64, 65]

$$K_{\parallel}^2 = (g_{\parallel} - 2.0023)\Delta E_{xy}/8\lambda_o \quad (3)$$

$$K_{\perp}^2 = (g_{\perp} - 2.0023)\Delta E_{xz}/2\lambda_o \quad (4)$$

$$K^2 = (K_{\parallel}^2 + 2K_{\perp}^2)/3 \quad (5)$$

Where λ_o is the spin orbit coupling of the free copper(II) ion (-828 cm^{-1}), ΔE_{xy} and ΔE_{xz} are the electronic transitions $^2B_{1g} \rightarrow {}^2B_{2g}$ and $^2B_{1g} \rightarrow {}^2E_g$ respectively. The calculated values of $k_{\parallel}^2$, $k_{\perp}^2$ and k^2 are in the 0.62-0.76, 0.55-0.64 and 0.76-0.82 ranges respectively Table 1. The data showed that, $K_{\parallel}^2 < K^2$ which is a good evidence for the assumed $^2B_1$ ground state for the complexes. Furthermore, for ionic environment, K = 1, and for covalent environment k is less than 1. The lower values of k than the unity (0.76-0.82) are indicative of their covalent nature, which in agreement with the conclusion obtained from the values of $g_{\parallel}$.[64, 65] The value of in plane sigma bonding parameters α^2 was calculated from the following equation (6)

$$\alpha^2 = (g_{\parallel} - 2.0023) + \frac{3}{7}(g_{\perp} - 2.0023) - \left(\frac{A_{\parallel}}{P}\right) + 0.04 \quad (6)$$

where P is the free ion dipolar term equals 0.036, $A_{\parallel}$ is the parallel coupling constant expressed in cm^{-1}. If the M-L bond is purely ionic the value of α^2 is unity and it is completely covalent, but if α^2 equal to 0.5. The α^2 values of the copper complexes **(2-4)** lie in the range 0.67-0.70, indicating to a significant degree of covalency in σ-plan.[63, 66, 67] Also, the in-plane and out-of plane π-bonding coefficients β◎and γ◎can be calculated using the following equations (7-8).

$$\alpha^2\gamma^2 = K_{\perp}^2 \quad (7)$$

$$\alpha^2\beta^2 = K_{\parallel}^2 \quad (8)$$

The copper(II) complexes **(2)** and **(4)** show β^2 values equal to 1.05 and 1.08 indicating ionic bond character in the in-plane π bonding while complex **(3)** shows β^2 equal 0.93 indicating a moderate degree of covalency in the in-plane π bonding. Also, these complexes show γ^2 in the 1.04-1.25 range respectively, indicating ionic bond character in the out-of-plane◎π bonding.[34, 68]The ESR spectra of the solid copper(II) complexes (**5**) at room temperature show nonaxial type symmetry with three g-values g_x = 2.24, g_y= 2.124, and g_z = 2.067. $(g_y-g_z)/(g_x-g_y) < 1$ (= 0.491), indicating a $d_{(x2-y2)}$ ground state with covalent bond character.[69-71]

Table 1: - ESR parameters of Cu(II) complexes (2-5)

Complex No.	(2)	(3)	(4)	(5)
$g_{\parallel}/g_x$	2.277	2.262	2.248	2.240
$g_{\perp}/g_y$	2.047	2.05	2.045	2.124
g_{iso}/g_z	2.124	2.12	2.112	2.067
$A_{\parallel} \times 10^{-4}$ (cm^{-1})	128	137	131	--
$A_{\perp} \times 10^{-4}$ (cm^{-1})	33	24	29	--
$A_{iso} \times 10^{-4}$ (cm^{-1})	63	59	62	--
$g_{\parallel}/A_{\parallel}$ (cm-1)	178.5	164.7	171	--
G	5.9	5.27	5.64	--
ΔE_{xy}(cm^{-1})	15748	19342	16666	--
ΔE_{xz} (cm^{-1})	20408	22222	23041	--
$K_{\parallel}^2$	0.65	0.76	0.62	--
$K_{\perp}^2$	0.55	0.64	0.58	--
K^2	0.58	0.68	0.59	--
K	0.76	0.82	0.77	--
α^2	0.69	0.7	0.67	--
β^2	1.05	0.93	1.08	--
γ^2	1.25	1.04	1.12	--

[a] $g_{iso} = (2g_{\perp}+g_{\parallel})/3$ [b] $G = (g_{\parallel}-2)/(g_{\perp}-2)$

3.8. Thermal analysis of some complexes

Thermal degradation of metal complexes **(3), (5), (8)** and **(10)** were studied in the range of 50–1000 ˚C to elucidate the nature of water molecules in theses complexes. The solid complexes were stable at room temperature and decompose gradually with the formation of respective metal oxides. The complexes thermo-behavior showed a good weight loss agreement between the calculated and found values Table 2. Complex **(3)** decomposed in two stages. The first one occurred in 130-200 °C with 3.41% weight losses (calcd. 3.27%) corresponding to loss of a coordinated water molecule. The second step occurred in range 228-412 °C with 87.50% weight loss (calcd 89.52%) represents the complete degradation of complexes ending with metal oxide formation (CuO). Complex **(5)** decomposed in three steps. The first step occurred in the temperature range 50-110 °C accompanied with 2.76% weight losses (calcd. 3.02%) corresponding to removal of two coordinated water molecules. The second step occurred in the temperature range 140-270 °C which was accompanied by 10.59 % weight losses (calcd. 10.40 %) corresponding to the elimination the HNO_3. The third stage occurred in the temperature range 270-470 °C accompanied with 74.85 weight losses (calcd. 79.9%) corresponding to the complete degradation of the complex ending up with formation of CuO. Complexes **(8)** shows four-stage decomposition process. Firstly, elimination of hydrated water molecules occurred in the temperature range 50-92 °C with 2.92%

IJSER

weight loss (calcd. 2.67%). Secondly elimination of coordinated water molecules occurred in (175-208) °C range with 5.84% weight loss (calcd. 5.35 %). The third step occurred 244-308 °C range with 8.44 % weight loss (calcd. 8.83 %) corresponding to the elimination the anions (CH_3COOH). The forth step took place 344-505 °C range with 72.1 % weight loss (calcd. 72.02 %) points out to the total degradation of complexes ending up with the formation of CoO. Complex **(10)** decomposed in two stages. The first one occurred in 140-238 °C with 17.06% weight losses (calcd. 17.33%) corresponding to loss of two acetate ions. The second step occurred in range 250-519 °C with 69.41% weight loss (calcd 70.81%) represents the complete degradation of complexes ending with metal oxide formation (ZnO).

Table 2. The thermal analysis (TG) of some complexes

No.	Temp. range °C	Found (calcd.)	Composition of the residue
(3)	130-200	3.41(3.27)	$[Cu(H_4L)_2]$
	228-412	87.50(89.52)	CuO
(5)	50-110	2.76(3.02)	$[Cu(H_5L)_2(NO_3)_2]$
	140-270	10.59(10.40)	$[Cu(H_5L)_2]$
	340-530	74.85(79.9)	CuO
(8)	50-92	2.92 (2.67)	$[Co(H_4L)(CH_3COO)(H_2O)_2]$
	175-208	5.84 (5.35)	$[Co(H_4L)(CH_3COO)]$
	244-308	8.44(8.83)	$[Co(H_4L)]$
	344-505	72.1(72.02)	CoO
(10)	140-238	17.06(17.33)	$[Zn(H_5L)]$
	250-519	69.41(70.81)	ZnO

3.9. Antimicrobial studies

The standardized disc-agar diffusion method [34] was followed to determine the microbicide activity of the synthesized compounds against fungi as *A. flavus and S. cerevisiae* as well as bacteria like *E. coli* and *B. subtili*. The screening data were presented in Table 3. The result showed that synthesized compounds are more active against Fungi than bacteria. However, the MIZ values of the compounds revealed that the compounds **(1-6) and (11-14)** have higher activity with MIZ, mm (AI, %) in range 15(125)-30(250) against *A. flavus* and their activity are more than standard antifungal drug (Nystatin). The most active compound is Hg(II) complex **(12)** with MIZ, mm (AI, %) 30(250). The screening data of the compounds against *S. cerevisiae* revealed that only complexes **(2-6), (8), (11)** and **(12)** with MIZ, mm (AI, %) in range 11(79)-32(229). The MIZ values of these complexes revealed that the most active complexes against are *S. cerevisiae* **(11)** which exhibit antifungal activity (MZI, mm (AI, %) = 32(229%). Moreover, the complexes **(2-6), (8), (12)** have high antifungal activity more than standard antifungal drug (Nystatin). with MIZ in the 15-27 mm range with activity index ranged between 107% to 193%, in comparing with Nystatin 14(100). The order of antibacterial activity of the compounds against fungal strains are shown in Fig. 7. Otherwise, the antibacterial screening data revealed that all compounds have moderate to low activity against all bacteria strain used (E. coli and B. subtilis) with MIZ ranged between 10-35 mm with AI in the range 20-88 %. However, the most active compound is complex **(12)** with MIZ equal the activity of antibacterial standard drug (tetracycline) 50 (100%) against *E. coli.* The order of antibacterial activity of the compounds against fungal strains are shown in Fig. 8. The enhancement in the potent antifungal and antibacterial activities of the complexes seems to be due to increment of lipophilic character of these complexes which could be explained based on Overtone's concept [72, 73] and Tweedy's Chelation theory.[73, 74] Based on Overtone's concept of cell permeability, the liposoliobility is an important factor in which the lipid material can pass through the lipid cell membrane, which manages the antifungal activity. The positive charge on the metal ion decreased largely due to electron donor groups on the ligand as well as overlap with ligand orbitals, which cause a decrease in the metal ion polarity. Furthermore, the lipophilicity can be enhanced by increasing the delocalization of π-electrons over the ligand rings. This lead to enhance the complex penetration through the cell membrane and blocking of the metal binding sites in the enzymes of microorganisms. As a result, deactivate various cellular enzymes, which play an important role in metabolic pathways of these microorganisms. It is also suggested that the function of the toxicant is the product of natural analogue of one or more proteins of the cell, which as a result, impairs the normal cellular processes.

Table 3. Results of antimicrobial bioassay of ligand and its complexes (concentration used 1mg/mL of DMSO), *A. flatus, S. cerevisiae,* E *coli* and *B. subtilis*

No.	Inhibition zone (MIZ, mm) and Activity Index (AI, %)							
	A. flavus		*S.*		*E. coli*		*B. subtilis*	
	MIZ	AI	MIZ	AI	MIZ	AI	MIZ	AI
DMSO	0	0	0	0	0	0	0	0
Nystatin	12	100	14	100	--	--	0	0
Tetracy-	--	--			50	100	40	100
(1)	15	125	0	0	10	20	13	33
(2)	15	125	20	143	13	26	23	58
(3)	16	133	15	107	14	28	12	30
(4)	19	158	25	179	16	32	35	88
(5)	22	183	25	179	14	28%	22	55
(6)	16	133	22	157	23	46	24	60
(7)	0	0	0	0	12	24	30	75
(8)	11	92	27	193	17	34	25	63
(9)	10	83	0	0	11	22	16	40
(10)	10	83	0	0	17	34	20	50
(11)	15	125	32	229	20	40	33	83
(12)	30	250	19	136	50	100	26	65
(13)	17	142	11	79	26	52	22	55
(14)	18	150	0	0	11	22	15	38

CONCLUSION

We have synthesized Fe(III), Co(II), Ni(II), Cu(II), Zn(II), Ag(I), Cd(II), Hg(II) and ZrO(II) complexes of a hydrazonic polydentate ligand, 2-benzylidene) hydrazono)ethyl)phenyl)ethylidene) hydrazono)ethyl)-2,4-dihydroxyphenyl)ethan-1-one under mild conditions. The ligand and the new complexes were characterized using; IR, thermal analysis, NMR, MS, molar conductivity, magnetic moment or ESR measurements. The data of various analyses revealed that the ligand chelated to the metal ions as a neutral or monobasic bidentate fashion

IJSER

through azomethine nitrogen, protonated/deprotonated hydroxyl group of a salicyl moiety forming an octahedral or distorted octahedral geometry around the centre metal ions. All prepared compounds were screened against *A. flavus, S. cerevisiae, B. subtilis and E. coli.* The prepared compounds are more active against Fungi than bacteria. the promising active compounds against *A. flavus,* are complexes **(1-6) and (11-14)** while complexes **(2-6), (8) and (11-13)** active against *S. cerevisiae*. These results encourage to synthesizing more complexes from a hydrazonic ligand with salicyl moiety in the future.

REFERENCES

1. I. Dasna, S. Golhen, L. Ouahab, M. Fettouhi, O. Pena, N. Daro, J.-P. Sutter, Inorg. Chim. Acta **2001**, 326, 37.
2. S. N. Subhendu Naskar, Ray J. Butcher, Shyamal Kumar Chattopadhyay, in 'Synthesis and spectroscopic properties of Ni(II) complexes of some aroyl hydrazone ligands with 2,6-diacetyl pyridine monooxime: X-ray crystal structure of the salicyloylhydrazone Ni(II) complex', Elsevier, Amsterdam, PAYS-BAS, 2010.
3. F. A. El-Saied, M. M. Abd-Elzaher, A. S. El Tabl, M. M. E. Shakdofa, A. J. Rasras, Beni-suef Uni. J. Basic and Appl. Sci. **2017**, 6, 24.
4. C. Anitha, C. D. Sheela, P. Tharmaraj, S. Sumathi, Spectrochim. Acta Part A Mol. Biomol. Spectrosc. **2012**, 96, 493.
5. M. K. Sahani, U. Yadava, O. P. Pandey, S. K. Sengupta, Spectrochim. Acta Part A Mol. Biomol. Spectrosc. **2014**, 125, 189.
6. R. R. Zaky, K. M. Ibrahim, I. M. Gabr, Spectrochim. Acta Part A Mol. Biomol. Spectrosc. **2011**, 81, 28.
7. Y. Dong, R. K. Narla, E. Sudbeck, F. M. Uckun, J. Inorg. Biochem. **2000**, 78, 321.
8. A. C. González-Baró, V. Ferraresi-Curotto, R. Pis-Diez, B. S. Parajón Costa, J. A. L. C. Resende, F. C. S. de Paula, E. C. Pereira-Maia, N. A. Rey, Polyhedron **2017**, 135, 303.
9. F. A. El-Saied, T. A. Salem, M. M. E. Shakdofa, A. N. Al-Hakimi, A. S. Radwan, Beni-suef Uni. J. Basic and Appl. Sci. **2017**.
10. F. A. El-Saied, M. M. E. Shakdofa, A. S. El-Tabl, M. M. A. Abd-Elzaher, Main Group Chem. **2014**, 13, 87.
11. A. S. El-Tabl, M. M. E. Shakdofa, A. M. E. Shakdofa, J. Serb. Chem. Soc. **2013**, 78, 39.
12. G. Svehla, in 'Vogel's textbook of macro and semi micro Quantitative inorganic analysis fifth Ed', Longman Inc: New York, 1979.
13. F. Welcher, Princeton, Von Nostrand **1958**.
14. A. Vogel, 'A Text Book of Quantitative Inorganic Analysis', ELBS, London, 1978.
15. Z. Holzbecher, L. Divis, M. Kral, in 'Handbook of organic reagents in inorganic analysis', John Wiley, 1976.
16. B. Figgis, J. Lewis, R. Wilkins, Interscience, New York **1960**, 403.
17. W. J. Geary, Coord. Chem. Rev. **1971**, 7, 81.
18. L. A. Baeva, L. F. Biktasheva, A. A. Fatykhov, N. K. Lyapina, Russ. J. Org. Chem. **2013**, 49, 1283.
19. C. P. Pandhurnekar, E. M. Meshram, H. N. Chopde, R. J. Batra, Org. Chem. Inter. **2013**, 2013, 1.
20. H. R. Fatondji, S. Kpoviessi, F. Gbaguidi, J. Bero, V. Hannaert, J. Quetin-Leclercq, J. Poupaert, M. Moudachirou, G. C. Accrombessi, Med. Chem. Res. **2013**, 22, 2151.
21. M. R. Maurya, S. Agarwal, C. Bader, D. Rehder, Eur. J. Inorg. Chem. **2005**, 147.
22. M. R. Maurya, S. Khurana, C. Schulzke, D. Rehder, Eur. J. Inorg. Chem. **2001**, 779.
23. O. Pouralimardan, A. C. Chamayou, C. Janiak, H. Hosseini-Monfared, Inorg. Chim. Acta **2007**, 360, 1599.
24. R. Gup, B. Kirkan, Spectrochim. Acta Part A Mol. Biomol. Spectrosc. **2005**, 62, 1188.
25. M. F. R. Fouda, M. M. Abd-Elzaher, M. M. Shakdofa, F. A. El-Saied, M. I. Ayad, A. S. El Tabl, J. Coord. Chem. **2008**, 61, 1983.
26. M. F. R. Fouda, M. M. Abd-Elzaher, M. M. E. Shakdofa, F. A. El Saied, M. I. Ayad, A. S. El Tabl, Transition Met. Chem. **2008**, 33, 219.
27. G. Y. Nagesh, B. H. M. Mruthyunjayaswamy, J. Mol. Struct. **2015**, 1085, 198.
28. A. Jayamani, V. Thamilarasan, N. Sengottuvelan, P. Manisankar, S. K. Kang, Y. I. Kim, V. Ganesan, Spectrochim. Acta Part A Mol. Biomol. Spectrosc. **2014**, 122, 365.
29. B. N. Bessy Raj, M. R. P. Kurup, Spectrochim. Acta Part A Mol. Biomol. Spectrosc. **2007**, 66, 898.
30. V. D. Biradar, B. H. M. Mruthyunjayaswamy, Sci. World J. **2013**, 2013.
31. M. Shebl, S. M. E. Khalil, A. Taha, M. A. N. Mahdi, Spectrochim. Acta Part A Mol. Biomol. Spectrosc. **2013**, 113, 356.
32. M. Shebl, Spectrochim. Acta Part A Mol. Biomol. Spectrosc. **2009**, 73, 313.
33. K. Nakamoto, 'Infrared and Raman Spectra of Inorganic and Coordination Compounds Part B: Applications in Coordination, Organometallic, and Bioinorganic Chemistry', John Wiley & Sons INC, USA, 2009.
34. A. S. El-Tabl, M. M. E. Shakdofa, M. A. Whaba, Spectrochim. Acta Part A Mol. Biomol. Spectrosc. **2015**, 136, 1941.
35. K. Nakamoto, J. Fujita, S. Tanaka, M. Kobayashi, J. Am. Chem. Soc. **1957**, 79, 4904.
36. B. M. Gatehouse, S. E. Livingstone, R. S. Nyholm, J. Chem. Soc. **1957**, 4222.
37. E. Katsoulakou, V. Bekiari, C. P. Raptopoulou, A. Terzis, P. Lianos, E. Manessi-Zoupa, S. P. Perlepes, Spectrochim. Acta Part A Mol. Biomol. Spectrosc. **2005**, 61, 1627.
38. S. Chandra, L. K. Gupta, Spectrochim. Acta Part A Mol. Biomol. Spectrosc. **2005**, 61, 2549.
39. Z. H. A. El-Wahab, M. M. Mashaly, A. A. Salman, B. A. El-Shetary, A. A. Faheim, Spectrochim. Acta Part A Mol. Biomol. Spectrosc. **2004**, 60, 2861.
40. A. N. Al-Hakimi, A. M. A. Alkwlini, M. M. E. Shakdofa, S. O. M. A. asbahi, F. A. Elsaied, M. A. Wahba, J. Nat. Sci. Math. **2017**, 10, 1.
41. F. A. El-Saied, M. M. E. Shakdofa, A. S. E. Tabl, M. M. Abd-Elzaher, N. Morsy, Beni-suef Uni. J. Basic and Appl. Sci. **2017**, 6, 310.

IJSER

42. S. Chandra, L. K. Gupta, Spectrochim. Acta Part A Mol. Biomol. Spectrosc. **2004**, 60, 1563.
43. S. Chandra, S. Gautam, H. K. Rajor, R. Bhatia, Spectrochim. Acta Part A Mol. Biomol. Spectrosc. **2015**, 137, 749.
44. A. A. El-Bindary, A. Z. El-Sonbati, Polish J. Chem. **2000**, 74, 615.
45. A. B. P. Lever, 'Inorganic electronic spectroscopy', Elsevier science, Amsterdam 1984.
46. A. A. A. Emara, A. A. Saleh, O. M. I. Adly, Spectrochim. Acta Part A Mol. Biomol. Spectrosc. **2007**, 68, 592.
47. A. S. El-Tabl, F. A. Aly, M. M. E. Shakdofa, A. M. E. Shakdofa, J. Coord. Chem. **2010**, 63, 700.
48. S. Xiao-Hui, Y. Xiao-Zeng, L. Cun, X. Ren-Gen, Y. Kai-Be, Transition Met. Chem. **1995**, 20, 191.
49. S. Chandra, A. Kumar, Spectrochim. Acta Part A Mol. Biomol. Spectrosc. **2007**, 68, 1410.
50. S. Chandra, S. Sharma, Transition Met. Chem. **2007**, 32, 150.
51. A. S. El-Tabl, R. M. El-Bahnasawy, M. M. E. Shakdofa, A. E. D. A. Ibrahim Hamdy, J. Chem. Res. **2010**, 88.
52. S. L. Reddy, T. Endo, G. S. Reddy, 'Electronic (Absorption) Spectra of 3d Transition Metal Complexes, Advanced Aspects of Spectroscopy', InTech, 2012.
53. M. Sönmez, Turk. J. Chem. **2001**, 25, 181.
54. A. Guha, J. Adhikary, T. Kumar Mondal, D. Das, Indian J. Chem. Sect. A Inorg. Phys. Theor. Anal. Chem. **2011**, 50, 1463.
55. G. A. Bain, J. F. Berry, J. Chem. Educ. **2008**, 85, 532.
56. F. A. El-Saied, T. A. Salem, M. M. E. Shakdofa, A. N. Al-Hakimi, Appl. Organomet. Chem. **2018**, 32.
57. D. R. Brown, D. X. West, J. Inorg. Nucl. Chem. **1981**, 43, 1017.
58. K. Nagashri, J. Joseph, C. J. Dhanaraj, Appl. Organomet. Chem. **2011**, 25, 704.
59. A. A. G. Tomlinson, B. J. Hathaway, J. Chem. Soc. A: Inorg. Phys. Theo. **1968**, 1685.
60. M. Shebl, J. Mol. Struct. **2017**, 1128, 79.
61. A. A. G. Tomlinson, B. J. Hathaway, J. Chem. Soc. A: Inorg. Phys. Theo. **1968**, 1905.
62. A. N. Al-Hakimi, A. S. El-Tabl, M. M. E. Shakdofa, J. Chem. Res. **2009**, 770.
63. D. Kivelson, R. Neiman, J. Chem. Phys. **1961**, 35, 149.
64. R. K. Ray, G. B. Kauffman, Inorg. Chim. Acta **1990**, 174, 257.
65. R. K. Ray, G. B. Kauffmann, Inorg. Chim. Acta **1990**, 174, 237.
66. P. B. Sreeja, M. R. P. Kurup, A. Kishore, C. Jasmin, Polyhedron **2004**, 23, 575.
67. B. Swamy, J. R. Swamy, Transition Met. Chem. **1991**, 16, 35.
68. A. S. El-Tabl, Bulletin of the Korean Chemical Society **2004**, 25, 1757.
69. A. S. El-Tabl, M. M. E. Shakdofa, A. M. A. El-Seidy, A. N. Al-Hakimi, Phosphorus Sulfur Silicon Relat. Elem. **2012**, 187, 1312.
70. J. M. Dance, M. T. D. P. Gambardella, R. H. D. A. Santos, E. Medina, F. G. Manrique, M. S. Palacios, Inorg. Chim. Acta **1989**, 162, 239.
71. V. T. Kasumov, F. Köksal, Spectrochim. Acta Part A Mol. Biomol. Spectrosc. **2012**, 98, 207.
72. Y. Anjaneyulu, R. P. Rao, Synth. React. Inorg. Met-Org. Chem. **1986**, 16, 257.
73. R. S. Joseyphus, M. S. Nair, Mycobiology **2008**, 36, 93.
74. N. Dharmaraj, P. Viswanathamurthi, K. Natarajan, Transition Met. Chem. **2001**, 26, 105.

IJSER